Acoustics of porous media with inner resonators

Claude Boutin[a)]
Ecole Nationale des Travaux Publics de l'Etat, Université de Lyon, DGCB - CELYA - UMR CNRS 5513, 69518 Vaulx-en-Velin Cedex, France

(Received 1 November 2012; revised 16 May 2013; accepted 28 May 2013)

This paper deals with the acoustics of rigid porous media with inner resonators both saturated by the same gas. The aim is to define porous media microstructures in which inner resonance phenomena may occur, and to provide the modeling of acoustic waves in this situation. The first part, focuses on the design of a periodic medium consisting in damped Helmholtz resonators embedded in a porous matrix. In the second part, the macroscopic description of this system is established through the homogenization method. In the third part, the features of acoustic wave propagation are determined, and the occurrence of a broad band gap along with strongly dispersed waves is discussed according to the characteristics of the porous matrix and of the damped resonators.
 [http://dx.doi.org/10.1121/1.4824965]

PACS number(s): 43.20.Jr, 43.20.Bi, 43.20.Ks, 43.20.Fn [KVH] Pages: 4717–4729

I. INTRODUCTION

This paper focuses on acoustic waves in rigid porous media with embedded inner resonators both saturated by the same gas. The present study deals with materials that present a statistically invariant representative volume element, that are conveniently represented by periodic media.

The idea is to enforce a "partial" non-equilibrium state at the local scale. Indeed, heterogeneous media, presenting such a local state are driven at the macroscopic scale by non-conventional mechanics. Among various examples, let us mention the local resonance in highly contrasted elastic composites evidenced in the pioneer paper,[1] demonstrated in practice[2–4] and analyzed mathematically;[5,6] or the transient inner diffusion in double porosity media[7,8] experimentally evidenced in poro-acoustics.[9] Weakly damped resonance (quasi-elastic composites) or strongly damped resonance (diffusion mechanisms) yield different macroscopic modeling (with or without inner-resonance band gaps frequencies, respectively). However, their common feature is that their macroscopic description strongly departs from usual modeling. Such materials, currently named "metamaterials," are of prime interest for their unconventional properties, that are seemingly impossible to reach with classical materials.

We investigate heterogeneous porous media where long wavelength Λ coincide with some local resonance in the period. The scale separation between the macroscopic characteristic length of the wave $L = \Lambda/2\pi$, and the period size ℓ, introduces the small scale ratio parameter $\varepsilon = 2\pi\ell/\Lambda = \ell/L \ll 1$ and enables the use of the homogenization method to derive the macroscopic description by means of multiple scale expansions.[10,11] The phenomena differ (1) from Rayleigh scattering (where wavelengths are slightly longer than the period, hence local dynamic effects are weak),[12,13] and (2) from Bragg scattering at high frequency in periodic media (where wavelengths are comparable to the period size),[14] e.g., see Refs. 15 and 16. In this latter case, periodic media can be described through Floquet–Bloch theory,[17,18] multiscattering approach[19] or by asymptotic method as in elastic composites[20] or in porous media.[21]

The aim of this paper is twofold: First, define microstructures of heterogeneous porous media in which inner resonance phenomena may occur, and second, provide the modeling of acoustic waves in this situation. The first part, focuses on the design of a periodic medium consisting in damped Helmholtz resonators embedded in a porous matrix. In the second part, the macroscopic description of this system is established through the homogenization method. In the third part, the features of acoustic wave propagation are determined, and the occurrence of a broad band gap along with strongly dispersed waves is discussed according to the characteristics of the matrix and of the resonators.

II. HETEROGENEOUS RIGID POROUS MEDIA WITH INNER RESONANCE

A. Conditions for "co-dynamics" regime

In heterogeneous media, the coexistence of dynamic phenomena at both micro and macro scales, named here after "co-dynamics," is a situation that only occurs with specific microstructural configurations. In usual elastic composites or single porosity media, when the macroscopic wavelength is much larger than the Representative Elementary Volume (REV), the whole cell experiences a quasi-static equilibrium state. Conversely, inner resonance means that, a sub-domain of the cell experiences a dynamic state [the resonating component(s)], while the complementary domain experiences a quasi-static state and acts as conveyor for the long wavelength [the carrying component(s)]. According to the physics in consideration the requirements for "co-dynamics" differ. Nevertheless, since a macroscopic phenomenon remains, these situations can be handled through the homogenization method.[10,11] It is useful to recall briefly the cases of elastic meta-material,[1,22] and of double porosity media.[7,8]

a)Author to whom correspondence should be addressed. Electronic mail: claude.boutin@entpe.fr

1. General considerations

In elastic composites, the distinct roles of the constituents imposed by "co-dynamics" entail that the carrying constituent is considerably much stiffer than the resonating constituent (when the density of the constituents are of the same order).[1,2,22] Further, the stiff domain must be connected meanwhile the soft resonating domain may be either connected or unconnected. At the leading order, the stress state is determined by the stiff constituent that moves at the cell scale in uniform motion. This uniform motion is imposed to the boundary of the soft constituent. In this latter, because of the dynamic "elasto-inertial" regime, the motion is not uniform and depends on the frequency. As a consequence, the mean inertia of the REV is also frequency dependent and the effective apparent density reaches infinite values (positive or negative) at the eigen-frequencies of the resonating constituent. In practice, the singularities are regularized by the presence of a weak damping. The inner resonance induces narrow band-gaps centered around the eigen-frequencies of the soft domain. These band gaps are of different nature than those related to diffraction at high frequency in periodic systems, since they occur here at large wavelength.

In gas saturated rigid double porosity media, "co-dynamics" imposes the carrying constituent to be far more permeable than the resonating constituent.[8,9,23] The very permeable domain must be connected, but the weakly permeable domain may be either connected or unconnected. At the leading order, the gas flux is determined by the permeable constituent that undergoes at the cell scale an uniform pressure. This uniform pressure is imposed to the boundary of the weakly permeable domain. In this latter, the mass transfer through permeability is balanced by the gas compressibility. This introduces a "permeo-compression" dynamic state, and it ensues that the pressure is not uniform and depends on the frequency. Hence, when considering the global mass balance, the effective compressibility is frequency dependent. However, conversely to the "elasto-inertia" resonance, the "permeo-compression" resonance driven by viscosity is highly damped. Therefore, no band-gap occurs, yet a significant increases of dissipation appears in a wide frequency band centered around the frequency for which the "permeo-compression" characteristic size is on the order of the size of the weakly permeable domain.

The composite and double porosity cases evidence that a "co-dynamics" regime requires that the flux (of stress or mass) induced by the resonating domain is sufficiently small to be negligible at the leading order (so that the effective constitutive parameters are on the order of those of the carrying constituent), but also sufficiently large to contribute to the macroscopic balance (as a source term for the carrying constituent). In this asymmetric interaction, the resonating domain undergoes a dynamic forced regime imposed by the carrying constituent.

As inner resonance is a general concept, it applies to different physics as electromagnetism, heat transfer, bubbly fluids,…. Hence, parallels can be established between these several fields. In elastic composite, the forcing variable is the motion and the inner resonance induces frequency dependent density; in double porosity media, the forcing variable is the pressure, and the inner resonance induces frequency dependent compressibility. Similarly, for the widely studied electromagnetic metamaterials, in media of highly contrasted electric permittivity (respectively, magnetic permeability), the forcing variable is the electromagnetic (respectively, electric) field and inner resonance results in frequency dependent magnetic permeability (respectively, electric permittivity).[24]

For each physics, the practical conditions to reach this phenomenon differ and need a specific study. A particularity of the poro-acoustics case, is that instead of using highly contrasted constituents, it is sufficient to introduce a "geometrical contrast" in the microstructure to create a resonating domain behaving as an Helmholtz resonator.

2. Porous media with inner resonators

To investigate "co-dynamics" with "elasto-inertia" resonance in porous media, we consider a periodic 3D medium, of period $\hat{\Omega}$, constituted by a rigid single porosity matrix (carrying constituent) with embedded Helmholtz resonators (Fig. 1), both domains being saturated by air. For simplicity, the period is assumed to contain a single Helmholtz resonator Ω_h that does not intercept the boundary $\partial\hat{\Omega}$ of the period. The period $\hat{\Omega}$, the resonator Ω_h, and the porous matrix domain Ω, present a common characteristic size ℓ, and the concentration of resonators is $c = |\Omega_h|/|\hat{\Omega}|$.

The porous matrix presents pores much smaller than ℓ (this condition is not mandatory; cf. Sec. III C 3). Thus, at the scale of the period, the matrix is described by the classic poro-acoustics as derived phenomenologically,[25–29] or by homogenization.[8,11]

The resonator Ω_h is made of a "chamber" $\tilde{\Omega}$ and a constricted "duct" Ω' both delimited by a thin impervious rigid surface $\tilde{\Gamma}$ and Γ'. The duct is of length $\ell' = O(\ell)$ and its constant section Σ (aperture on the matrix) and $\tilde{\Sigma}$ (aperture on the chamber) is much smaller than that of the period, i.e., $|\Sigma|/\ell^2 \ll 1$, so that the duct volume $|\Omega'| = O(|\Sigma|\ell)$ is negligible compared to $|\tilde{\Omega}|$, and $|\tilde{\Omega}| \approx |\Omega_h|$. For convenience, the duct is assumed to be located inside the chamber so that the interface Γ between the porous matrix and the resonator is $\Gamma = \tilde{\Gamma} \cup \Sigma$. Figure 1 depicts a configuration with an

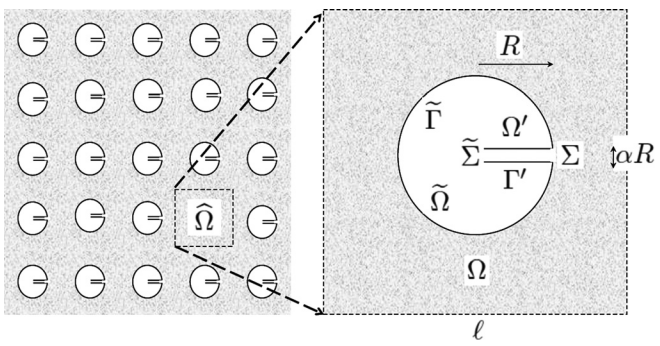

FIG. 1. (Left) Porous matrix with periodically embedded spherical Helmholtz resonators. (Right) Period of the media with spherical Helmholtz resonator.

Helmholtz resonator made of a spherical cavity of radius R with a duct of length R having a radius αR, $\alpha \ll 1$.

A key condition for having a "co-dynamics" regime lies in the geometrical contrast between $|\Sigma|$ and ℓ^2. This is traduced mathematically by setting $|\Sigma| = O(\varepsilon\ell^2)$, i.e., the section of the duct is 1 order smaller than the period section. With this geometrical constraint, the pressure that prevails in the matrix acts on the small aperture Σ and induces a flux pulsed by the resonator. With a velocity $\mathbf{v}'$ in the duct of the same order as the velocity $\mathbf{v}$ in the porous matrix, i.e., $O(|\mathbf{v}|) = O(|\mathbf{v}'|)$, the pulsed flux is of 1 order smaller than the flux carried through the matrix $O(|\mathbf{v}'||\Sigma|/|\mathbf{v}|\ell^2) = O(|\Sigma|/\ell^2) = \varepsilon \ll 1$. Nevertheless this flux contributes as a source to the mass balance of the gas in the matrix. This corresponds to a forced regime of the resonator, enabling the co-dynamics regime. In absence of geometric contrast, i.e., $|\Sigma| = O(\ell^2)$, the domain Ω_h would behaves as a large pore without resonance effect, and for extreme geometric contrast, i.e., $|\Sigma| \leq O(\varepsilon^2\ell^2)$, the source due to the resonator would be negligible in the mass balance at the leading order.

The second condition to have a "co-dynamics" regime is related to the permeability and is established in Sec. II B 2.

B. Physics at the local scale

We investigate small acoustic perturbations in the frequency range of long wavelength and dynamic regime in the resonators. The analysis is performed in the Fourier space with harmonic time dependence exp $(i\omega t)$ where ω and $f = \omega/2\pi$ are the angular frequency and the frequency. For air at ambient condition, the pressure and density at equilibrium are, respectively, $P^e = 1.013\times10^5$Pa, $\rho^e = 1.2$kg/m^3; $\mathcal{C}^e = \sqrt{\gamma P^e/\rho^e} = 343$, 3 m/s is the sound velocity, $\gamma = 1.4$ the adiabatic coefficient, $\mu = 1.85 \times 10^{-5}$ Pa s the viscosity.

1. Helmholtz resonators

Each resonator responds to the perturbation of pressure P in the matrix according to the known "Helmholtz behavior." Because of the scale separation, the acoustic wavelength is much larger than the period, hence than the chamber size. Then, the gas in the chamber suffers a quasi-static and adiabatic compression (neglecting thermal transfer), which results in uniform perturbation of pressure $\tilde{P}$, different from P.

The pressure in the duct varies from P at the aperture Σ on the matrix, to $\tilde{P}$ at the aperture $\tilde{\Sigma}$ on the chamber. As the chamber $|\tilde{\Omega}|$ is much larger than the duct $|\Omega'|$, the volume variation in $|\Omega'|$ is negligible. Then, the gas mass $\rho^e|\Omega'|$ moves with a uniform motion u'. Thus a volume $u'|\Sigma|$ is injected in the chamber, that results in a perturbation of pressure: $\tilde{P} = \gamma P^e u'|\Sigma|/|\tilde{\Omega}|$. In turn, the mass undergoes a force $\tilde{P}|\Sigma|$, from which we deduce the equivalent spring of the gas chamber

$$\mathrm{k} = \frac{\tilde{P}|\Sigma|}{u'} = \frac{\gamma P^e|\Sigma|^2}{|\tilde{\Omega}|}.$$

The motion $\tilde{u}$ in the chamber is much smaller than the motion u' in the duct since $O(\tilde{u}/\ell) = O(\tilde{P}/\gamma P^e) = O(u'|\Sigma|/|\tilde{\Omega}|)$, and $O(\tilde{u}/u') = |\Sigma|/\ell^2 = \varepsilon \ll 1$.

Neglecting the viscous forces on the wall of the duct, the momentum balance equation for the mass in the duct submitted to P and $\tilde{P}$ on its extremities Σ and $\tilde{\Sigma}$, reads

$$(\tilde{P} - P)|\Sigma| = \rho^e|\Omega'|\frac{\partial^2 u'}{\partial t^2},$$
$$\text{i.e.,}\quad \mathrm{k}u' - \rho^e|\Omega'|\omega^2 u' = P|\Sigma|.$$

The eigen-frequency $f_0 = \omega_0/2\pi$ of the resonator results from the chamber compressibility and the duct inertia,

$$\omega_0 = 2\pi f_0 = \sqrt{\frac{\mathrm{k}}{\rho^e|\Omega'|}} = \frac{\mathcal{C}^e}{\delta}$$
$$\text{where}\quad \delta = \frac{\sqrt{|\tilde{\Omega}||\Omega'|}}{|\Sigma|} = O\left(\frac{\ell^2}{\sqrt{|\Sigma|}}\right). \tag{1}$$

Since $|\Sigma|/\ell^2 \ll 1$, then $\delta \gg \ell$ and the resonance occurs at a frequency much lower than diffraction frequency of the media $f_0 \ll f_d = \mathcal{C}^e/(2\pi\ell)$. In the situation described in Fig. 1,

$$\omega_0 = \mathcal{C}^e\frac{\sqrt{3}}{2}\frac{\alpha}{R},$$

and with a radius cavity of $R = 2$ cm and radius of duct of $\alpha R = 2$ mm, $f_0 \approx 236$ Hz. It is easy to verify that the viscosity effect on the moving mass in the duct is not significant. Indeed, the flow is governed by inertia for frequencies higher than the characteristic visco-inertial frequency $f_c' = \omega_c'/2\pi$. For a duct of radius αR

$$\omega_c' = \frac{8\mu}{\rho^e(\alpha R)^2},$$

$$\frac{\omega_0}{\omega_c'} = \frac{\mathcal{C}^e\rho^e}{\mu}\frac{\sqrt{3}}{8}\alpha^3 R \approx 2.4\times10^6\alpha^3 R.$$

With the same values as above, $\omega_0 \approx 50 \times \omega_c'$ which indicates dominant effects of inertia.

As mentioned previously, a weak amount of dissipation regularizes the behavior of the resonator. Therefore, in the following, the viscous dissipation in the duct will be taken into account. Furthermore, the possibility of increasing the dissipation will be considered by introducing a porous medium in the duct (see Sec. III C 3). In any case, the flow will be driven by a dominant inertia effect (i.e., $\omega_0 \geq \omega_c'$) as in usual Helmholtz resonators.

2. Porous matrix

At the period scale, the matrix of porosity ϕ_m is regarded as an equivalent homogeneous medium described by the classic poro-acoustics. For simplicity, the matrix is assumed isotropic and the dynamic permeability tensor and tortuosity tensor reduce to scalar functions K_m and $\tau_m = \mu/(i\omega\rho^e K_m)$. K_m, τ_m and the effective gas stiffness $E_m = (P^e/\phi_m)(1 - \Pi_m)^{-1}$, depend on the frequency. At low frequencies, the flow is driven by the viscosity, then $K_m \to \mathcal{K}_m$, the real-valued intrinsic permeability; and the

perturbation is quasi-isotherm so $E_m \to P^e/\phi_m$. Hence, in viscous regime, the wavelength is on the order of $\Lambda_m(\omega)/(2\pi) = O(\sqrt{\mathcal{K}_m P^e/(\omega\mu\phi_m)})$. At high frequencies, the flow is driven by the inertia, then $K_m \to (\phi_m\mu)/(i\omega\rho^e\alpha_{m_\infty})$, where α_{m_∞} is the high frequency limit of the tortuosity, and the perturbation is quasi-adiabatic, thus $E_m \to \gamma P^e/\phi_m$ and the wavelength in inertial regime is on the order of $\Lambda_m(\omega)/(2\pi) = O(\mathcal{C}^e/(\sqrt{\alpha_{m_\infty}}\omega))$. The two regimes are delimited by the critical frequency ω_c derived by equalizing the low frequency viscous effects and the high frequency inertial effects: $\omega_c = (\phi_m\mu)/(\mathcal{K}_m\rho^e\alpha_{m_\infty})$ [the isothermal/adiabatic transition occurs at a frequency $\omega_t = O(\omega_c)$].

Because of the scale separation, the pressure in the matrix varies at the macro (i.e., wavelength) scale and is therefore uniform in the period at the leading order. The velocity in the matrix is not uniform because of the conditions on the resonator surface Γ, i.e., impervious condition on $\tilde{\Gamma}$ and continuity of flux and pressure on the aperture surface Σ.

It is worth mentioning that the "co-dynamics" condition is naturally fulfilled when the resonance occurs at frequency corresponding to the inertial regime in the matrix, i.e., $\omega_0 > \omega_c$. Indeed, in this case $\Lambda_m(\omega 0)/(2\pi) = O(\mathcal{C}^e/(\sqrt{\alpha_{m_\infty}}\omega_0)) = \ell^2/\sqrt{|\Sigma|} \gg \ell$ [see (1)], that ensures the coexistence of local and global dynamics. From the expressions of ω_0 and ω_c this situation arises when

$$\frac{\mathcal{K}_m\alpha_{m_\infty}}{\phi_m} > \frac{\mu}{\rho^e\mathcal{C}^e}\delta = \frac{\mu}{\rho^e\mathcal{C}^e}O\left(\frac{\ell^2}{\sqrt{|\Sigma|}}\right).$$

Conversely, when the resonance occurs at frequency corresponding to the viscous regime in the matrix, i.e., $\omega_0 < \omega_c$, the "co-dynamics" condition is rather restrictive. Indeed, the scale separation condition $\Lambda_m(\omega_0)/(2\pi) \gg \ell$ reads in that case

$$\sqrt{\mathcal{K}_m P^e/(\omega\mu\phi_m)} \gg \ell.$$

The two inequalities leads to the following requirement for the permeability

$$\frac{\ell^2}{\delta}\frac{\alpha_{m_\infty}}{\gamma} \ll \frac{\mathcal{K}_m\alpha_{m_\infty}}{\phi_m}\frac{\rho^e\mathcal{C}^e}{\mu} < \delta.$$

That is also, dividing by ℓ and since $\alpha_{m_\infty}/\gamma = O(1)$, $\ell/\delta = \sqrt{|\Sigma|}/\ell = O(\sqrt{\varepsilon})$,

$$O(\sqrt{\varepsilon}) \ll \frac{\mathcal{K}_m\alpha_{m_\infty}}{\ell\phi_m}\frac{\rho^e\mathcal{C}^e}{\mu} < O\left(\frac{1}{\sqrt{\varepsilon}}\right)$$
$$\text{hence} \quad \frac{\mathcal{K}_m\alpha_{m_\infty}}{\ell\phi_m}\frac{\rho^e\mathcal{C}^e}{\mu} = O(1). \tag{2}$$

Consequently, both frequency ranges show that "co-dynamics" situations can be reached only when

$$\frac{\mathcal{K}_m\alpha_{m_\infty}}{\phi_m} \geq \frac{\mu}{\rho^e\mathcal{C}^e}O(\ell), \quad \text{i.e.,} \quad \omega_0/\omega_c \geq O(\ell/\delta), \tag{3}$$

which means that the porous matrix must be in inertial or visco-inertial regime, but not in almost purely viscous regime ($\omega_0/\omega_c \ll 1$).

III. ACOUSTICS OF POROUS MEDIA WITH INNER RESONANCE

As we consider wavelength Λ much longer than the size ℓ of the period, we take benefit of the small scale ratio $\varepsilon = 2\pi l/\Lambda = \ell/L \ll 1$ to introduce multiple scale expansions, and derive the macroscopic description by homogenization. The micro and macro scales introduce two sets of dimensionless 3D space variables, $\mathrm{x}/l = \mathbf{y}^*$ and $\mathrm{x}/L = \mathbf{x}^*$ associated to the variations at both scales, where x stands for the usual space variables. Equivalently, taking L as reference length, two 3D space variables, $\mathbf{y} = L\mathbf{y}^* = \varepsilon^{-1}\mathrm{x}$ and $\mathbf{x} = L\mathbf{x}^* = \mathrm{x}$ will be used, the usual derivative being then changed into $\varepsilon^{-1}\partial/\partial y + \partial/\partial x$. The homogenization process is achieved as usual.[10,11] The variables are expanded in power of ε, each term (specified by exponents in brackets) being $\hat{\Omega}$ periodic. The expansions are introduced in the equations rewritten with the two-scale derivatives and rescaled according to the physics. The terms of the same power in ε are identified, and the problems in series are solved until the equation governing the phenomena at the leading order is obtained.

A. Formulation of the problem at the local scale

The governing equations at the local scale are given below. The variables in each domain are the perturbation of pressure p and the velocity $\mathbf{v}$ [by linearity, the harmonic time dependence $\exp(i\omega t)$ is skipped]. In the duct, they are denoted by a prime, in the chamber by a tilde.

1. Porous matrix

The poro-acoustic description in the matrix reads

$$\begin{cases} \operatorname{div}(\mathbf{v}) + i\omega\dfrac{p}{P^e}\phi_m(1-\Pi_m) = 0 \quad \text{on } \Omega, \\ \mathbf{v} = -\dfrac{K_m}{\mu}\cdot\nabla p \quad \text{on } \Omega, \\ \mathbf{v}\cdot\mathbf{n} = 0 \quad \text{on } \tilde{\Gamma}; \quad \mathbf{v}\cdot\mathbf{n} = \mathbf{v}'\cdot\mathbf{n}, \quad p = p' \quad \text{on } \Sigma, \\ \mathbf{v},\ p,\ \hat{\Omega}\text{-periodic}. \end{cases} \tag{4}$$

In the porous matrix, the pressure p and the velocity $\mathbf{v}$ are expanded as

$$p(\mathbf{x},\mathbf{y}) = p^{(0)}(\mathbf{x},\mathbf{y}) + \varepsilon p^{(1)}(\mathbf{x},\mathbf{y}) + \cdots,$$
$$\mathbf{v}(\mathbf{x},\mathbf{y}) = \mathbf{v}^{(0)}(\mathbf{x},\mathbf{y}) + \varepsilon\mathbf{v}^{(1)}(\mathbf{x},\mathbf{y}) + \cdots.$$

As the pressure and density vary at the macroscale, these equations do not need to be rescaled when re-expressed with the double $(\mathbf{x},\mathbf{y})$ variable system, since L is the reference length. However, the fact that $|\Sigma| = O(\varepsilon\ell^2) = O(\varepsilon|\Gamma|)$ will be explicitly taken into account in the resolution.

2. Gas in the duct

In the duct, he governing equations of the compressible viscous gas in adiabatic regime are

$$\begin{cases} \mathrm{div}(\mathbf{v}') + i\omega\dfrac{p'}{\gamma P^e} = 0 \quad \text{on}\,\Omega', \\ \mu\mathbf{div}(\mathbf{D}(\mathbf{v}')) - \nabla p' = i\omega\rho^e\mathbf{v}' \quad \text{on}\,\Omega', \\ \mathbf{v}'\cdot\mathbf{n} = 0 \quad \text{on}\,\Gamma'; \quad \mathbf{v}'\cdot\mathbf{n} = \mathbf{v}\cdot\mathbf{n},\ p' = p \quad \text{on}\,\Sigma, \\ \mathbf{v}'\cdot\mathbf{n} = \tilde{\mathbf{v}}\cdot\mathbf{n},\ p' = \tilde{p} \quad \text{on}\,\tilde{\Sigma}, \end{cases} \tag{5}$$

where $\mathbf{D}(\mathbf{v})$ is the strain rate. The pressure and the velocity in the duct are of the same order as in the porous matrix and are expanded as

$$p'(\mathbf{x},\,\mathbf{y}) = p'^{(0)}(\mathbf{x},\,\mathbf{y}) + \varepsilon p'^{(1)}(\mathbf{x},\,\mathbf{y}) + \cdots,$$
$$\mathbf{v}'(\mathbf{x},\,\mathbf{y}) = \mathbf{v}'^{(0)}(\mathbf{x},\,\mathbf{y}) + \varepsilon\mathbf{v}'^{(1)}(\mathbf{x},\,\mathbf{y}) + \cdots.$$

As the pressure and shear forces vary in the duct, when re-expressed with the $(\mathbf{x},\ \mathbf{y})$ variables (recall that L is the reference length), the terms $\mu\mathbf{div}(\mathbf{D}(\mathbf{v}'))$ and $\nabla p'$ have to be rescaled as $\mu(\ell/L)^2\mathbf{div}(\mathbf{D}(\mathbf{v}')) = \mu\varepsilon^2\mathbf{div}(\mathbf{D}(\mathbf{v}'))$ and $\ell/L\nabla p' = \varepsilon\nabla p'$, respectively. Thus, the x-y-rescaled Navier–Stokes equation takes the following form:

$$\mu\varepsilon^2\mathbf{div}(\mathbf{D}(\mathbf{v}')) - \varepsilon\nabla p' = i\omega\rho^e\mathbf{v}' \quad \text{on}\,\Omega'. \tag{6}$$

3. Gas in the chamber

The same set of balance equations as for the duct applies for the chamber

$$\begin{cases} \mathrm{div}(\tilde{\mathbf{v}}) + i\omega\dfrac{\tilde{p}}{\gamma P^e} = 0; \ \ \mu\mathbf{div}(\mathbf{D}(\tilde{\mathbf{v}}) - \nabla\tilde{p} = i\omega\rho^e\tilde{\mathbf{v}} \ \ \text{on}\,\tilde{\Omega}, \\ \tilde{\mathbf{v}}\cdot\mathbf{n} = 0 \ \ \text{on}\,\tilde{\Gamma}\cup\Gamma'; \ \ \tilde{\mathbf{v}}\cdot\mathbf{n} = \mathbf{v}'\cdot\mathbf{n},\ \tilde{p} = p' \ \ \text{on}\,\tilde{\Sigma}. \end{cases} \tag{7}$$

The pressure in the chamber is of the same order as in the porous matrix. As for the velocity, we noticed in the previous section that $O(\tilde{u}/u') = O(\varepsilon)$. Hence, the expansions read

$$\tilde{p}(\mathbf{x},\,\mathbf{y}) = \tilde{p}^{(0)}(\mathbf{x},\,\mathbf{y}) + \varepsilon\tilde{p}^{(1)}(\mathbf{x},\,\mathbf{y}) + \cdots,$$
$$\tilde{\mathbf{v}}(\mathbf{x},\,\mathbf{y}) = \varepsilon\tilde{\mathbf{v}}^{(1)}(\mathbf{x},\,\mathbf{y}) + \cdots.$$

In the chamber, the shear forces vary at the local scale. Consequently, $\mu\mathbf{div}(\mathbf{D}(\tilde{\mathbf{v}}))$ is rescaled as $\mu\varepsilon^2\mathrm{div}(\mathbf{D}(\tilde{\mathbf{v}})$ and, the "x-y-rescaled" Navier-Stokes equation is

$$\mu\varepsilon^2\mathbf{div}(\mathbf{D}(\tilde{\mathbf{v}})) - \nabla\tilde{p} = i\omega\rho^e\tilde{\mathbf{v}} \quad \text{on}\,\Omega'. \tag{8}$$

B. Macroscopic description

As the scaling enables to match the "co-dynamics" situation, the requirement (3) is necessarily and implicitly satisfied in the sequel.

1. Resolution in the matrix

The first cell problem encountered in the matrix, derived from set (4) reads

$$\begin{cases} \mathrm{div}_y\left(-\dfrac{K_m}{\mu}\cdot\nabla_y p^{(0)}\right) = 0 \ \ \text{on}\ \ \Omega \\ -\left(\dfrac{K_m}{\mu}\cdot\nabla_y p^{(0)}\right)\cdot n = 0 \ \ \text{on}\,\tilde{\Gamma}\cup\Sigma; \ \ p^{(0)},\ \hat{\Omega}\text{-periodic}, \end{cases}$$

whose obvious solution is $p^{(0)}(\mathbf{x},\mathbf{y}) = P^{(0)}(\mathbf{x})$.

The next order, gives the cell problem driving pressure $p^{(1)}(\mathbf{x},\mathbf{y})$ and velocity $\mathbf{v}^{(0)}(\mathbf{x},\mathbf{y})$,

$$\begin{cases} \mathbf{v}^{(0)} = -\dfrac{K_m}{\mu}\cdot(\nabla_y p^{(1)} + \nabla_x p^{(0)}); \quad \mathrm{div}_y(\mathbf{v}^{(0)}) = 0 \quad \text{on}\ \Omega, \\ \mathbf{v}^{(0)}\cdot\mathbf{n} = 0 \quad \text{on}\,\tilde{\Gamma}; \quad \mathbf{v}^{(0)}\cdot\mathbf{n} = \mathbf{v}'^{(0)}\cdot\mathbf{n} \quad \text{on}\ \Sigma, \\ p^{(1)}\hat{\Omega}\text{-periodic}. \end{cases}$$

The equivalent weak formulation is established by multiplying the balance equation by a test pressure field $\mathrm{p}(\mathbf{y})\,\hat{\Omega}$-periodic. Integrating over Ω and using the divergence theorem gives

$$-\int_\Omega\left(\frac{K_m}{\mu}\cdot(\nabla_y p^{(1)} + \nabla_x P^{(0)})\right)\cdot\nabla_y \mathrm{p}d\Omega = \int_{\partial\hat{\Omega}}\mathbf{v}^{(0)}\cdot\mathbf{n}\mathrm{p}ds + \int_{\tilde{\Gamma}}\mathbf{v}^{(0)}\cdot\mathbf{n}\mathrm{p}ds + \int_\Sigma\mathbf{v}^{(0)}\cdot\mathbf{n}\mathrm{p}ds.$$

On the right hand side, the two first integrals vanish because of the periodicity on $\partial\hat{\Omega}$ and the impervious boundary conditions on $\tilde{\Gamma}$. As for the last term, since $|\Sigma| = O(\varepsilon|\Gamma|)$, its contribution is $O(\varepsilon)$ relatively to the left hand side terms, and therefore can be disregarded at the considered order. Consequently, $p^{(1)} = p*^{(1)}(1 + O(\varepsilon))$, where $p*^{(1)}$ is the solution of the variational problem

$$\forall p(y) \qquad \hat{\Omega}\text{-periodic}, \int_\Omega\left(\frac{K_m}{\mu}\cdot\nabla_y p^{*(1)}\right)\cdot\nabla_y p d\Omega = -\int_\Omega\left(\frac{K_m}{\mu}\cdot\nabla_x P^{(0)}\right)\cdot\nabla_y p d\Omega.$$

This is a problem of conduction through a matrix with non-conducting inclusions. As K_m is uniform, the problem is purely geometric. The solution reads

$$p^{*(1)} = \boldsymbol{\xi}(\mathbf{y})\cdot\nabla_x P^{(0)}(\mathbf{x}),$$

where the three components of $\boldsymbol{\xi}(\mathbf{y})$ are the particular real-valued solutions for unit pressure gradient in three directions.[10] The local flux reads $\mathbf{v}^{(0)} = \mathbf{v}^{*(0)}(1 + O(\varepsilon))$, where

$$\mathbf{v}^{*(0)}(\mathbf{x},\mathbf{y}) = -\frac{K_m}{\mu}(\nabla_y\boldsymbol{\xi} + \mathbf{I})\cdot\nabla_x P^{(0)}.$$

The difference of order 1, $\mathbf{v}^{(0)} - \mathbf{v}^{*(0)} = O(\varepsilon\mathbf{v}^{*(0)}) = \varepsilon\mathbf{w}^{(1)}$ stems from the flux (unknown up to now) pulsed by the resonator, i.e., $q^{(1)} = \int_\Sigma\mathbf{v}'^{(0)}.\mathbf{n}ds$. It contributes to the cell problem at the next order only.

At the leading order, the mass balance in Ω, given by (4) reads [$\mathbf{w}^{(1)}$ is included in $\mathbf{v}^{(1)}$]

$$\mathrm{div}_y(\mathbf{v}^{(1)}) + \mathrm{div}_x(\mathbf{v}^{*(0)}) + i\omega\frac{P^{(0)}}{P^e}\phi_m(1 - \Pi_m) = 0.$$

Integrating over Ω and using the divergence theorem and the periodicity condition gives

$$\int_\Gamma \mathbf{v}^{(1)}\cdot\mathbf{n}ds+\int_\Omega \mathrm{div}_x(\mathbf{v}^{*(0)})d\Omega + i\omega\frac{P^{(0)}}{P^e}\phi_m(1-\Pi_m)|\Omega|=0.$$

The integral on Γ is the flux $q^{(1)}$ exchanged between the matrix and the resonator, i.e.,

$$\int_\Gamma \mathbf{v}^{(1)}\cdot\mathbf{n}ds=q^{(1)}=\int_\Sigma \mathbf{v}'^{(0)}\cdot\mathbf{n}ds. \tag{9}$$

Introducing the macro flux $\mathbf{V}^{(0)}$ and the macroscopic dynamic permeability tensor $\mathbf{K}=K_m\mathbf{A}$ ($\mathbf{A}$ is a real tensor that depends only on the geometry of the matrix in the period),

$$\mathbf{V}^{(0)}=\frac{1}{|\hat\Omega|}\int_\Omega \mathbf{v}^{*(0)}d\Omega;\quad \mathbf{A}=\frac{1}{|\hat\Omega|}\int_\Omega(\nabla_y\boldsymbol{\xi}+\mathbf{I})d\Omega,$$

the mean mass balance on the matrix and the dynamic Darcy law read

$$\frac{1}{|\hat\Omega|}q^{(1)}+\mathrm{div}_x(\mathbf{V}^{(0)})+i\omega\frac{P^{(0)}}{P^e}\phi_m(1-\Pi_m)\frac{|\Omega|}{|\hat\Omega|}=0;$$
$$\mathbf{V}^{(0)}=-\frac{K_m}{\mu}\mathbf{A}\cdot\nabla_x P^{(0)}. \tag{10}$$

To go further we have to determine the flux $q^{(1)}$ exchanged with the resonator.

2. Resolution in the duct

The velocity and pressure at the leading order, are driven by the set (5) modified with the re-scaled Navier-Stokes Eq. (6). To simplify the presentation, we directly introduce the fact that the pressure at the leading order in the chamber is uniform, of value $\tilde P^{(0)}(\mathbf{x})$, as demonstrated independently in the next paragraph,

$$\begin{cases}\mathrm{div}_y(\mathbf{v}'^{(0)})=0 \quad \text{on}\,\Omega',\\ \mu\Delta_y(\mathbf{v}'^{(0)})-\nabla_y p'^{(0)}=i\omega\rho^e\mathbf{v}'^{(0)} \quad \text{on}\,\Omega',\\ \mathbf{v}'^{(0)}\cdot\mathbf{n}=0 \quad \text{on}\,\Gamma',\\ p'^{(0)}=P^{(0)} \quad \text{on}\,\Sigma;\qquad p'^{(0)}=\tilde P^{(0)} \quad \text{on}\,\tilde\Sigma.\end{cases}$$

This set describes a visco-inertial incompressible flow forced by the imposed pressures at the extremities of the duct and the velocity is in the form

$$\mathbf{v}'^{(0)}(\mathbf{x},\mathbf{y})=-\frac{\zeta(\omega,\mathbf{y})}{i\omega\rho^e}\frac{\tilde P^{(0)}-P^{(0)}}{\ell'}.$$

The flux $q^{(1)}$ defined by (9), constant along the duct because of $\mathrm{div}_y(\mathbf{v}'^{(0)})=0$, reads

$$q^{(1)}=\int_\Sigma \mathbf{v}'^{(0)}\cdot\mathbf{n}ds=-\frac{|\Sigma|}{i\omega\rho^e\tau'(\omega)}\frac{\tilde P^{(0)}-P^{(0)}}{\ell'}, \tag{11}$$

where $\tau'(\omega)$ is the dynamic tortuosity of the duct defined by

$$\tau'(\omega)=\left[\frac{1}{|\Sigma|}\int_\Sigma\zeta(\omega,\mathbf{y})\cdot\mathbf{n}ds\right]^{-1}.$$

If the duct is a straight cylinder of circular section of radius αR, the frequency dependent tortuosity $\tau(\omega)$ involves Bessel functions[30]

$$\tau'(\omega)=\frac{J_0(i\sqrt{i8\omega/\omega_c'})}{J_2(i\sqrt{i8\omega/\omega_c'})};\quad \omega_c'=\frac{8\mu}{\rho^e(\alpha R)^2},$$

and when the flow is dominated by the inertia, i.e., $\omega/\omega_c'\gg 1$, $\tau'(\omega)$ can be approximated as

$$\tau'(\omega)\approx 1+\frac{1}{\sqrt{2i\omega/\omega_c'}}\quad\text{when}\quad \omega/\omega_c'\gg 1\,. \tag{12}$$

Remember that expression (11) applies only when requirement (3) is satisfied.

It is here worth to underline that, conversely to the situation of a single resonator in a open space, where the incident field and the scattered field are naturally separated, the periodic distribution of the oscillator makes that the scattered fields interact and contribute to the pressure field at the leading order. Thus the separation into incident and scattered fields is not directly related to the asymptotic process: $P^{(0)}$ involves both the "incident pressure" and the mean part of the field resulting form the interferences of the periodic scattered field. Note also that the small attenuation due to the radiation of the pressure at the vicinity of the aperture is not accounted for at the leading order considered here.

3. Resolution in the chamber

The first equation derived from (8) is $\nabla_y\tilde p^{(0)}=0$ and therefore $\tilde p^{(0)}(\mathbf{x},\mathbf{y})=\tilde P^{(0)}(\mathbf{x})$. Consequently, at the leading order the mass balance gives

$$\mathrm{div}_y(\tilde{\mathbf{v}}^{(1)})+i\omega\frac{\tilde P^{(0)}}{\gamma P^e}=0.$$

Integrating this equation over $\tilde\Omega$ and using the divergence theorem and the impervious condition on $\tilde\Gamma$ and Γ' gives (the normal of the chamber is the opposite of the normal of the duct)

$$-q^{(1)}+i\omega\frac{\tilde P^{(0)}}{\gamma P^e}|\tilde\Omega|=0. \tag{13}$$

For this result, it is sufficient to formulate the global flux balance on $\tilde\Sigma$ without appeals to the point to point velocity continuity. In fact, the velocity in the duct is of an order higher than in the chamber and a transition zone in the vicinity of the duct enables the matching of both fields. In practice, this region is on the order of the duct's radius and may be disregarded in a leading order description.

C. Homogenized model

Equating the flux $q^{(1)}$ derived in the duct (11) and in the chamber (13) provides

$$i\omega\frac{\tilde{P}^{(0)}}{\gamma P^e}|\tilde{\Omega}| = -\frac{|\Sigma|}{i\omega\rho^e\tau'(\omega)}\frac{\tilde{P}^{(0)}-P^{(0)}}{\ell'}.$$

Thus, for straight duct where $|\Omega'| = |\Sigma|\ell'$,

$$\left(1-\omega^2\tau'(\omega)\frac{\rho^e}{\gamma P^e}\frac{|\tilde{\Omega}||\Omega'|}{|\Sigma|^2}\right)\tilde{P}^{(0)} = P^{(0)}. \tag{14}$$

Therefore, recalling that $\omega_0 = \mathcal{C}^e|\Sigma|/\sqrt{|\tilde{\Omega}|\,|\Omega'|}$,

$$q^{(1)} = i\omega\frac{P^{(0)}}{\gamma P^e}\frac{|\tilde{\Omega}|}{1-(\omega/\omega_0)^2\tau'(\omega)}.$$

Reporting this result in the mass balance equation established for the matrix (10), leads to the leading order set of equations (remind that $1-c = |\Omega|/|\hat{\Omega}|$), valid up to a precision ε,

$$\begin{cases} \mathrm{div}_x\left(\mathbf{V}^{(0)}\right) + i\omega\dfrac{P^{(0)}}{\gamma P^e}\left(\phi_m(1-c)\gamma(1-\Pi_m(\omega)) + \dfrac{c}{1-(\omega/\omega_0)^2\tau'(\omega)}\right) = 0 \\ \mathbf{V}^{(0)} = -\dfrac{K_m(\omega)}{\mu}\mathbf{A}\cdot\nabla_x P^{(0)}. \end{cases} \tag{15}$$

This set constitutes the macroscopic description, where the effective dynamic permeability and compressibility are deduced from the knowledge of the microstructure. This formulation accounts for the "co-dynamic" regime in the media, with the simultaneous occurrence of macroscopic wave-length and local dynamics in the resonator that arises when the condition (3) is satisfied. This situation involves two distinct pressure fields at the period scale, namely, $P^{(0)}$ that "carries" the macroscopic wave, and $\tilde{P}^{(0)}$ developed in the resonator as forced response to $P^{(0)}$.

1. Effective dynamic permeability

The effective dynamic permeability is that of the matrix corrected by the real valued tensor $\mathbf{A}$. The effective permeability is the same as if the resonators were impervious inclusions, and therefore is reduced compared to the permeability of the matrix. For period geometry presenting three orthogonal planes of symmetry, the macroscopic tensor is isotropic, i.e., $\mathbf{A} = A\mathbf{I}$. Using classical results on conduction in heterogeneous media,[31] we necessarily have $A < 1-c$ and for spherical resonators at a concentration $c \le 1/3$, A can be assessed quite accurately by $A \approx 2(1-c)/(2+c)$.

2. Effective stiffness

The frequency dependent effective stiffness $E(\omega)$ is significantly modified compared to that prevailing in usual porous media. It reads

$$E(\omega) = \gamma P^e\left(\phi_m(1-c)\gamma(1-\Pi_m(\omega)) + \frac{c}{1-(\omega/\omega_0)^2\tau'(\omega)}\right)^{-1}.$$

For the physical interpretation, it is easier to reformulate $E(\omega)$ as

$$E(\omega) = \left(\frac{1-c}{E_m}+\frac{c}{E_r}\right)^{-1};$$
$$E_m(\omega) = (P^e/\phi_m)(1-\Pi_m(\omega))^{-1};$$
$$E_r(\omega) = \gamma P^e(1-(\omega/\omega_0)^2\tau'(\omega)).$$

The geometric mean discloses an association *in series* 1 of the effective gas stiffness in the matrix E_m and 2 of the apparent stiffness E_r that reflects the elasto-inertial nature of the resonator, each being weighted by the volume ratio of its respective domain.

In absence of dissipation $\tau'(\omega) = 1$ and E_r decreases continuously with the frequency

$$E_r(\omega \ll \omega_0) \to \gamma P^e; \quad E_r(\omega_0) = 0;$$
$$E_r(\omega > \omega_0) < 0; \quad E_r(\omega \gg \omega_0) \to -\infty.$$

The un-conventional properties of the effective stiffness are simply evidenced in the case where $\omega_0 > \omega_c$ (and $\omega_0 > \omega_t$) so that the thermal behavior is adiabatic and $E_m(\omega_0) \approx \gamma P^e/\phi_m$. Then

$$E(\omega) \approx E_1(\omega) = \gamma P^e\left((1-c)\phi_m + \frac{c}{1-(\omega/\omega_0)^2}\right)^{-1}$$

that is negative in the frequency band $[\omega_0, \omega_0^*]$ designated as "atypical band" in the sequel

$$\omega_0^* = \omega_0\sqrt{1+\frac{c}{(1-c)\phi_m}},$$
$$E_1(\omega) \ge 0 \quad \text{if} \quad \omega \notin [\omega_0, \omega_0^*]; \quad E_1(\omega_0) = 0,$$
$$E_1(\omega) \le 0 \quad \text{if} \quad \omega \in [\omega_0, \omega_0^*]; \quad E_1(\omega_0^{*\pm}) = \pm\infty. \tag{16}$$

More generally, in the frequency range of the resonator effect, say $[(1/2)\,\omega_0, 2\omega_0^*]$, the effective behavior of the gas differs radically from its usual behavior in porous media. Note that if the matrix is in isothermal regime around ω_0, the upper limit of the atypical band becomes $\omega_0\sqrt{1+(c/(1-c)\phi_m)\gamma}$.

The dissipation regularizes the behavior, but nevertheless a strong effect of the resonator remains. Introducing the weak dissipation in $\tau'(\omega)$ as in (12) yields

$$E_r(\omega) = \gamma P^e \left(1 - (\omega/\omega_0)^2 \left(1 + \frac{1}{\sqrt{2i\omega/\omega'_c}}\right)\right).$$

The visco-inertial nature of the dissipation leads to an unusual damped response function involving a term as $\omega^{3/2}/\sqrt{i}$. At the resonance, $E_r(\omega_0) = -(\gamma P^e)/\sqrt{2i\omega_0/\omega'_c}$, so $|E_r(\omega_0)| \ll \gamma P^e/c$, since $\omega_0/\omega'_c \gg 1$. Consequently, considering again the adiabatic case where $E_m(\omega_0) \approx \gamma P^e/\phi_m$,

$$\begin{cases} E(\omega_0) \approx -\dfrac{\gamma P^e}{c}\dfrac{1}{\sqrt{2i\omega_0/\omega'_c}}, \\ E(\omega_0^*) \approx \dfrac{\gamma P^e}{c}\left(\dfrac{c\phi_m}{1-c}\right)^2\left(\dfrac{\omega_0}{\omega_0^*}\right)^2\sqrt{2i\omega_0^*/\omega'_c}, \\ \text{i.e., } |E(\omega_0)| \ll \dfrac{\gamma P^e}{c};\ |E(\omega_0^*)| \gg \dfrac{\gamma P^e}{c}. \end{cases} \tag{17}$$

The contrast between both values decreases as ω_0/ω'_c decreases, i.e., as the resonator's dissipation increases.

3. Other possible microstructure inducing inner resonance

Let us mention several variations (Fig. 2) of the studied configuration, that lead to a macro description of the same kind as (15). In any cases, the aspect ratios of the resonator geometry are kept: small section and volume of the duct compared to those of the chamber, in order to ensure that the resonating effect induces a small flux compared to the macroscopic flux. However, the chamber can take various form, sphere, ellipsoid, cubes, polyhedrons,….

The duct can be replaced by a device enhancing the dissipation. For instance, Ω' can be filled by N ducts of smaller diameters and infinitesimal thickness. The formulation is identical, however the critical frequency ω'_c involved in $\tau'(\omega)$ is increased by a factor $O(N)$. Ducts of corrugated boundary can also be contemplated in order to increase the damping and also the apparent inertia (i.e., $\tau'(\omega \to \infty) > 1$). This objective can also be achieved by introducing a porous media in Ω'. The theoretical treatment will be very close, replacing the local Navier-Stokes equations by a local poro-acoustic description. For a straight duct, the result is the replacement in (15) of $\tau'(\omega)$ by $\tau'^*(\omega)/\phi'$ where $\tau'^*(\omega)$ and ϕ' are the dynamic tortuosity and porosity of the media inserted in Ω'.

One may also suppress the porous matrix: either the frame of the medium is made by the resonators themselves and Ω consists in the inter-resonators pores, or some resonators are introduced in a impervious granular skeleton with grain's size of the same order as the resonator's size. In both cases, the theory would require to replace the poro-acoustic formulation in the matrix by a Navier-Stokes formulation of the gas flow in the pores Ω. However, as the resonator's flow is 1 order smaller that the pore's flow, impervious conditions at the pores/resonator interface apply at the leading order and lead to the classic Darcy dynamic problem.[32,33] Thus, one obtains a description of the same nature, except that K and Π are directly defined from the pores geometry Ω.

In these different cases, one may also insert in a period N resonators tuned with different frequencies. The effective stiffness then becomes: $E(\omega) = ((1-c)/E_m + \Sigma_{i=1}^N c_i/E_{r_i})^{-1}$, and the global effect affect a frequency band involving the resonant frequencies of each resonators.

Finally, similar homogenized description applies if *identical* resonators are non-periodically distributed. Indeed, when a separation of scales exists, i.e., for long wavelengths, periodic materials and non-periodic materials with REV show macroscopic behavior of the same nature.[11]

IV. ANALYSIS OF WAVE PROPAGATION

A. Feature of acoustic wave propagation

In the whole section we focus on macroscopic isotropic media. Eliminating the velocity in (15), and introducing the dynamic tortuosity of the matrix gives the following harmonic wave equation:

$$\begin{aligned} &-\frac{\phi_m A}{i\omega\rho^e\tau_m(\omega)}\Delta_x P^{(0)} + i\omega\frac{P^{(0)}}{E(\omega)} = 0, \\ &\text{i.e., } E(\omega)\Delta_x P^{(0)} + \omega^2\rho^e\frac{\tau_m(\omega)}{\phi_m A}P^{(0)} = 0. \end{aligned} \tag{18}$$

1. Acoustic wave velocity

Consider an harmonic plane wave $P^{(0)} = P \exp[i(\omega t - k(\omega)x)]$, of complex wave number $k(\omega)$. Reporting $P^{(0)}$ in (18), yields the complex and frequency dependent wave velocity $\mathcal{C}(\omega)$

$$\mathcal{C}(\omega) = \frac{\omega}{k(\omega)} = \sqrt{\frac{E(\omega)\phi_m A}{\rho^e\tau_m(\omega)}},$$

that is, explicitly,

$$\mathcal{C}(\omega) = \mathcal{C}^e\sqrt{\frac{A}{(1-c)}}\sqrt{\frac{1}{\tau_m(\omega)}\left(\gamma[1-\Pi_m(\omega)] + \frac{c}{\phi_m(1-c)}\frac{1}{1-(\omega/\omega_0)^2\tau'(\omega)}\right)^{-1}}.$$

The wave is characterized by its wavelength, $\Lambda = |C(\omega)|(2\pi/\omega)$ and the nature of the field (more or less attenuated or oscillating) defined by $\varphi(\omega) = Arg(\mathcal{C}(\omega))$. Far from the resonance, we obtain the limit behaviors

$$\text{when} \quad \omega/\omega_0 \ll 1, \quad \mathcal{C}(\omega) \approx \mathcal{C}^e \sqrt{\frac{A}{(1-c)}} \sqrt{\frac{1}{\tau_m(\omega)} \left(\gamma[1-\Pi_m(\omega)] + \frac{c}{\phi_m(1-c)} \right)^{-1}}, \tag{19}$$

which corresponds to the adiabatic participation of the gas in the chamber to the effective stiffness, and a dynamic permeability reduced by the form factor A;

$$\text{when} \quad \omega/\omega_0 \gg 1, \quad \mathcal{C}(\omega) \approx \mathcal{C}^e \sqrt{\frac{A}{(1-c)}} \sqrt{\frac{1}{\tau_m(\omega)\gamma(1-\Pi_m(\omega))}}, \tag{20}$$

which is the behavior that would be obtained if the resonators were impervious.

2. Atypical features: Dispersion and band gaps

A comprehensive analysis of the velocity can not be handled analytically, because of the complex value of the macro-parameters. However, the main features can be point out by assuming an adiabatic regime in the matrix, so that E_m becomes $\gamma P^e \phi_m$ Then, the velocity simplifies in $\mathcal{C}^\gamma(\omega)$,

$$\mathcal{C}^\gamma(\omega) = \mathcal{C}^\gamma_m(\omega) \sqrt{\left(1 + \frac{c}{\phi_m(1-c)} \frac{1}{1-(\omega/\omega_0)^2 \tau'(\omega)} \right)^{-1}}$$

$$\text{with } \mathcal{C}^\gamma_m(\omega) = \mathcal{C}^e \sqrt{\frac{A}{(1-c)}} \sqrt{\frac{1}{\tau_m(\omega)}}.$$

$\mathcal{C}^\gamma_m(\omega)$ is the velocity that would be obtained if the matrix were in adiabatic regime and if the resonators were impervious. It corresponds to a particular version of the classic poro-acoustic wave, and will be used in the sequel as reference model to highlights the effect of the resonators.

Frequency out of the atypical band, i.e., $0 \le \omega \le \omega_0$ or $\omega \ge \omega_0^*$. Let us, for the moment, neglect the resonator dissipation [taking $\tau'(\omega) = 1$ and denoting the velocity $\mathcal{C}^\gamma$ in this simplified case by $\mathcal{C}^\gamma_1$]. For those frequencies the effective stiffness is positive, and we simply have

$$\frac{\mathcal{C}^\gamma_1(\omega)}{\mathcal{C}^\gamma_m(\omega)} = R(\omega) = \sqrt{\left(1 + \frac{c}{\phi_m(1-c)} \frac{1}{1-(\omega/\omega_0)^2} \right)^{-1}};$$

$$Arg\,(\mathcal{C}^\gamma_1) = Arg(\mathcal{C}^\gamma_m).$$

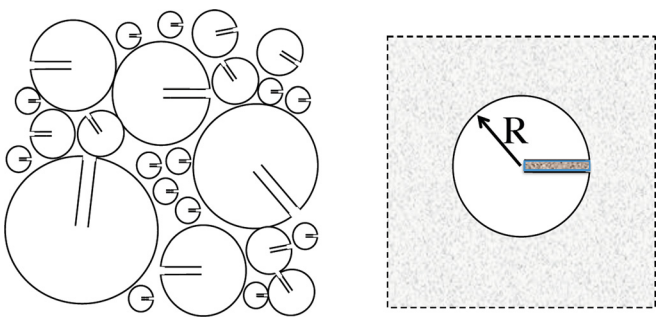

FIG. 2. (Color online) (left) Granular media made of Helmholtz resonators of different resonant frequency; (right) period made of a porous matrix with embedded Helmholtz resonator whose the duct enables enhanced damping.

Thus, the effect of resonators is to decrease (resp. increase) the velocity and the wavelength by $R(\omega)$ for $0 \le \omega \le \omega_0$ (respectively, $\omega \ge \omega_0^*$), keeping the nature the of waves identical as that of waves in the matrix. Frequencies ω_0 and ω_0^* lead to singular values: $\mathcal{C}^\gamma_1(\omega_0) = 0$ and $\Lambda(\omega_0) = 0$; $|\mathcal{C}^\gamma_1(\omega_0^{*\pm})| = \infty$ and $\Lambda(\omega_0^{*\pm}) = \infty$. These singularities are regularized by the resonator's damping. Taking $\tau'(\omega)$ given by (12) with $\omega_0/\omega'_c \gg 1$, yields the finite complex values

$$\mathcal{C}^\gamma(\omega_0) = \mathcal{C}^\gamma_m(\omega_0) \sqrt{\frac{\phi_m(1-c)}{c}} \frac{i}{\sqrt[4]{2i\omega_0/\omega'_c}};$$

$$\mathcal{C}^\gamma(\omega_0^*) = \mathcal{C}^\gamma_m(\omega_0^*) \sqrt{\frac{\phi_m(1-c)}{c}} \frac{\omega_0}{\omega_0^*} \sqrt[4]{2i\omega_0^*/\omega'_c}$$

that indicate a small finite wavelength at ω_0 and a large finite wavelength at ω_0^* (both compared to reference wavelength).

Frequency in the atypical band, i.e., $\omega_0 \le \omega \le \omega_0^*$. Considering first undamped resonators, taking $\tau'(\omega) = 1$ the effective stiffness takes real negative values and

$$\frac{\mathcal{C}^\gamma_1(\omega)}{\mathcal{C}^\gamma_m(\omega)} = \sqrt{\left| 1 + \frac{c}{\phi_m(1-c)} \frac{1}{1-(\omega/\omega_0)^2} \right|^{-1}};$$

$$Arg(\mathcal{C}^\gamma_1) = Arg(\mathcal{C}^\gamma_m) \pm \pi/2.$$

In usual porous media, as the argument of the dynamic tortuosity of the matrix varies from $-\pi/2$ at low frequency (viscous flow) to 0 at large frequency (inertial flow),[1] then $0 \le Arg\,(\mathcal{C}^\gamma_m) \le \pi/4$, and the wave is oscillating and damped as it progresses.

The $\pi/2$-jump of $Arg\,(\mathcal{C}^\gamma_1)$ in the atypical band modifies drastically the nature of the wave that becomes overdamped. Therefore, waves are confined in a region of characteristic size $\Lambda = |C(\omega)|(2\pi/\omega)$. Thus the atypical band corresponds to a band gap of the media.

Anomalous wave appear when $\varphi(\omega) > \pi/2$ or $\varphi(\omega) < 0$: The *phase* velocity is positive along with the wave amplitude amplifies in positive x direction. However, because of the negative effective stiffness, the group and phase velocities are of opposite sign. Therefore, the train of wave is actually attenuated when it propagates. This situation is similar to that encountered in 1D array of resonator.[33]

This analysis concerns only the situation of undamped resonator. In presence of damping the abrupt variations at ω_0 and ω_0^* are smoothed in a frequency zone where the real elastic term becomes smaller than the complex damped

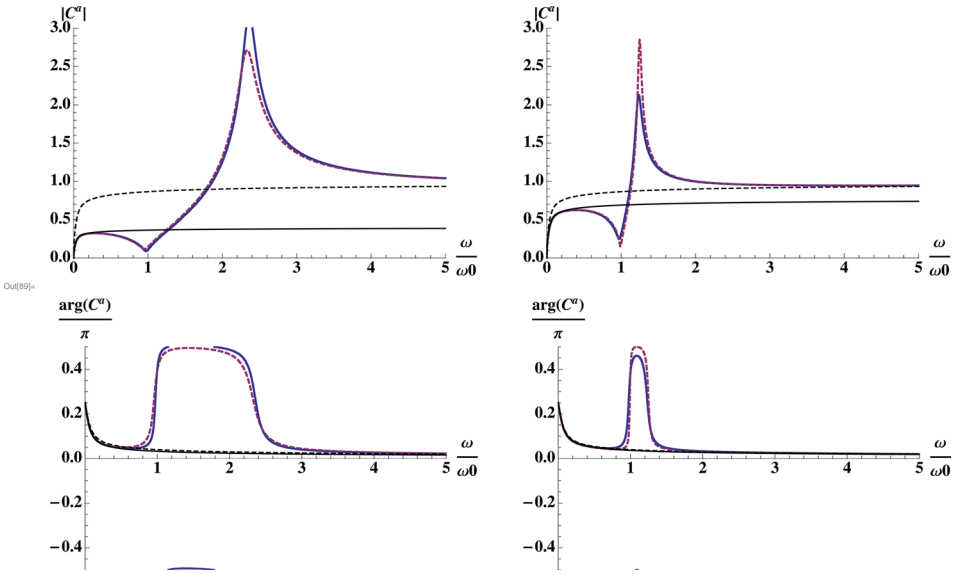

FIG. 3. (Color online) Dimensionless wave velocity $\mathcal{C}^{ad}(\omega)$ of a porous media with embedded resonators at concentration $c = 1/3$ with $\omega_0/\omega_c = 10$. (Top) Modulus and (bottom) phase versus dimensionless frequency ω/ω_0. Matrix of porosity (left) $\phi_m = 0.1$; (right) $\phi_m = 0.8$. Bold line: low damped resonator ($\omega_0/\omega'_c = 50$). Bold dashed line: resonator with enhanced damping, namely, $\omega_0/\omega'_c = 30$ for $\phi_m = 0.1$ (left); resonator with lower damping, namely, $\omega_0/\omega'_c = 800$ for $\phi_m = 0.8$ (right). For comparison, the characteristics of the single porosity media that match the low [Eq. (19)] and high [Eq. (20)] frequency behavior are drawn in normal and dashed lines.

term. Simple algebra gives the following assessment of the smoothing zones: $[\omega_0(1\pm\sqrt{\omega'_c/(8\omega_0)})]$ and $[\omega_0^*(1\pm(c\phi_m/(1-c))\sqrt{\omega'_c/(8\omega_0^*)})]$. One see that these zones are larger as the resonator's damping increases (i.e., ω_0/ω'_c decreases).[34,35]

B. Illustrating examples

To illustrate these results, Figs. 3–5 display the modulus and the argument of the dimensionless velocity $\mathcal{C}^a(\omega)$ versus the dimensionless frequency ω/ω_0, where

$$\mathcal{C}^a(\omega) = \sqrt{\frac{\alpha_{m_\infty}}{\tau_m(\omega)}\left(\gamma[1-\Pi_m(\omega)] + \frac{c}{\phi_m(1-c)}\frac{1}{1-(\omega/\omega_0)^2\tau'(\omega)}\right)^{-1}}.$$

Calculations are performed on porous media with embedded resonator at a concentration $c = 1/3$. Matrix of high porosity, $\phi_m = 0.8$, and low porosity, $\phi_m = 0.1$, are considered. The influence of the flow regime in the matrix at resonance is highlighted from the three cases: Dominant inertial flow $\omega_0/\omega_c = 10$, visco-inertial flow $\omega_0/\omega_c = 1$, and viscous flow with weak inertia $\omega_0/\omega_c = 0.1$ [this latter case is at the limit of applicability of the model, see (3)]. The effect of the dissipation of the resonator is also analyzed, by presenting the simple duct configuration ($\omega_0/\omega'_c = 50$ see Sec. II B 1), and in each case an adapted value of ω_0/ω'_c enabling to avoid anomalous waves in the atypical band. The dynamic tortuosity functions $\tau_m(\omega)$ and $\tau'(\omega)$, and the thermal permeability $\Pi_m(\omega)$ are approximated by the Johnson formula

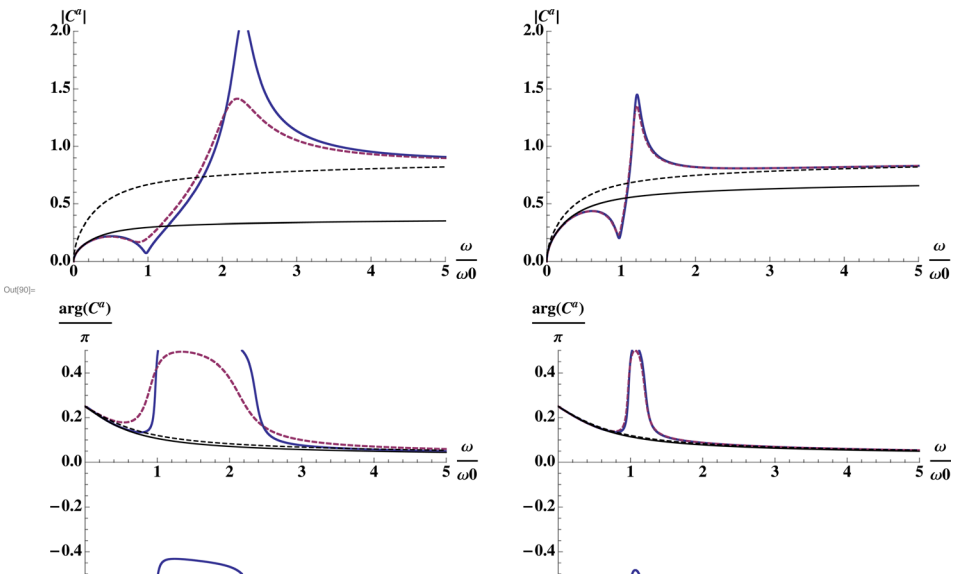

FIG. 4. (Color online) Same as Fig. 3 except that $\omega_0/\omega_c = 1$ and that the bold dashed lines correspond to resonators with enhanced damping (left) $\omega_0/\omega'_c = 4$ for $\phi_m = 0.1$ and (right) $\omega_0/\omega'_c = 60$ for $\phi_m = 0.8$.

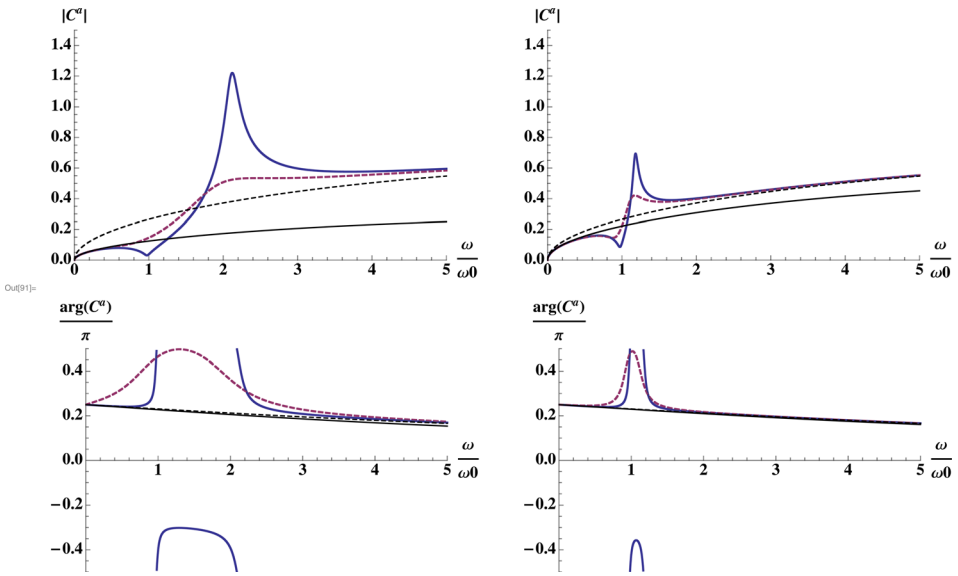

FIG. 5. (Color online) Same legend as Fig. 3 except that $\omega_0/\omega_c = 0.1$ and that the bold dashed lines correspond to damped resonator: (left) $\omega_0/\omega'_c = 1$ for $\phi_m = 0.1$; (right) $\omega_0/\omega'_c = 8$ for $\phi_m = 0.8$.

$$\frac{\tau_m(\omega)}{\alpha_{m_\infty}} = 1 + \frac{\omega_c}{i\omega}\sqrt{1 + \frac{M}{2}\frac{i\omega}{\omega_c}};$$

$$\frac{\tau'(\omega)}{\alpha'_\infty} = 1 + \frac{\omega'_c}{i\omega}\sqrt{1 + \frac{M'}{2}\frac{i\omega}{\omega'_c}};$$

$$\Pi_m(\omega) = \left(1 - \frac{1}{\gamma}\right)\left(1 + \frac{\omega_t}{i\omega}\sqrt{1 + \frac{M_t}{2}\frac{i\omega}{\omega_t}}\right)^{-1}$$

and to reduce the number of parameters, $\omega_t = \omega_c$, $M = M_t = 2$ for the porous medium and $M' = 1$, $\alpha'_\infty = 1$ for the ducts.

Figure 3 $(\omega_0/\omega_c = 10)$ shows that the influence of the resonators affect a broad frequency band, say $[\omega_0/2, 2\omega_0^*]$, where the acoustic wave presents a great dispersion. The role of the matrix porosity on the extent of the atypical frequency band is evident: for $\phi_m = 0.1$, $\omega_0^*/\omega_0 = 2.5$, and for $\phi_m = 0.8$, $\omega_0^*/\omega_0 \approx 1.3$. The high level of attenuation is focused in the band $[\omega_0,\ \omega_0^*]$, while the change of velocity appears in a much larger range, with low velocity when $\omega \leq \omega_0$ and high velocity when $\omega \geq \omega_0^*$. In the atypical band $[\omega_0, \omega_0^*]$ the "wave" is almost exponentially decaying $(\varphi \approx \pi/2)$, with a penetration depth of $|\mathcal{C}^a(\omega)|\omega$. A frequency band of large velocity and weak attenuation appears around $\omega \geq \omega_0^*$, specially with low porosity matrix. This may lead to acoustic wave propagating *faster* than in ambient air.

In the atypical band $[\omega_0, \omega_0^*]$, for low porosity matrix $\phi_m = 0.1$ and weakly damped configuration (simple duct, $\omega_0/\omega'_c = 50$), one observes anomalous waves, when $\mathrm{Arg}\,(\mathcal{C}^{ad}(\omega)) \approx -\pi/2$. Anomalous waves disappear by increasing the dissipation in the duct $(\omega_0/\omega'_c \leq 30)$. In the case of large porosity, a much smaller damping $(\omega_0/\omega'_c \leq 800)$ is sufficient to avoid anomalous waves.

The response of the medium presents a sharp band gap in the broad interval $[\omega_0,\ \omega_0^*]$ not centered on the tuned frequency ω_0. In Fig. 4, $(\omega_0/\omega_c = 1)$ similar trends are observed. The band gap is slightly shifted to lower frequency, not as sharp as in the case of Fig. 3, and the velocity is also smoothed. With low porosity, anomalous waves occurs in the atypical band with weakly damped resonators $(\omega_0/\omega'_c = 50)$ but disappears by increasing the dissipation $(\omega_0/\omega'_c \leq 4)$. For the high porosity matrix, the required damping is significantly lower $(\omega_0/\omega'_c = 70)$.

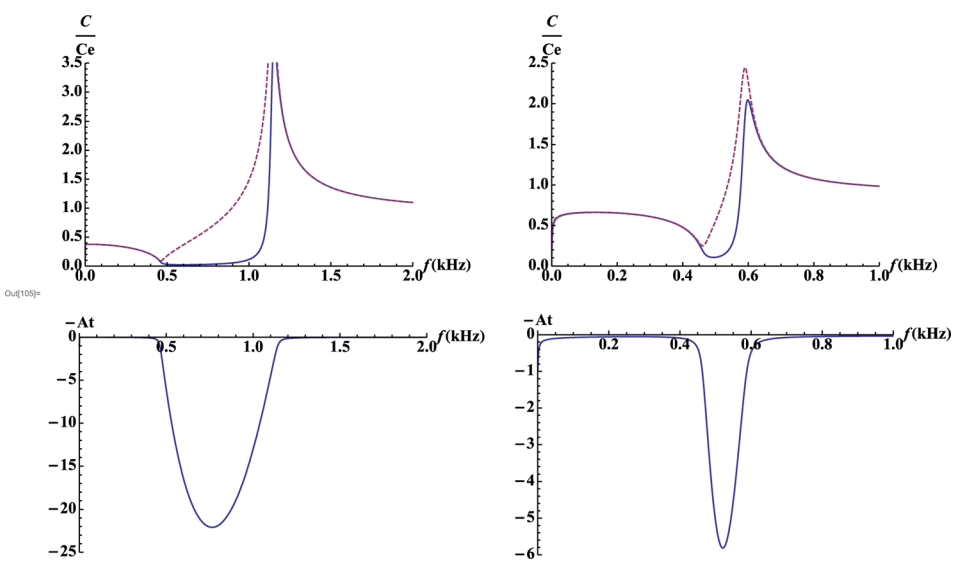

FIG. 6. (Color online) Wave characteristics versus frequency of resonator of eigen-frequency $f_0 = 473$ Hz embedded (left) in a dense fibrous media, and (right) in an open cell foam. (Top) Real part and Absolute value (dashed line) of the velocity divided by the sound velocity. (Bottom) Attenuation factor (presented with opposite value to enable correspondence with the velocity).

In Fig. 5, $(\omega_0/\omega_c = 0.1)$, presents the same qualitative trends. The atypical band give rise to anomalous diffusion wave. In this case, the resonator's damping needed to avoid this type of waves is much larger, respectively, $\omega_0/\omega'_c = 1$, $(\omega_0/\omega'_c = 8)$ for the low (high) porosity matrix case. The band gap remains localized around $[\omega_0,\ \omega_0^*]$ with high porosity matrix, while with low porosity matrix, velocity and attenuation are significantly modified in the whole low frequency band $[0,\ \omega_0^*]$.

Finally, Fig. 6 presents two realistic examples with resonators in concentration $c = 1/3$, of eigen-frequency $f_0 = 473$ Hz (radius cavity of $R = 1$ cm, radius of duct of $\alpha R = 1$ mm, simple duct configuration, i.e., $\omega_0/\omega'_c = 50$). In the first case, they are embedded in a dense fibrous material typical for thermal insulation, having a porosity $\phi_m = 0.1$ an intrinsic permeability $\mathcal{K}_m = 6.2 \times 10^{-5}\text{m}^2$, and a high frequency tortuosity $\alpha_{m_\infty} \simeq 1$, thus $\omega_c = 2.5 \times 10^{-2}$ Hz. With these values $\omega_0/\omega_c = 125$ and the atypical band gap is $[f_0 = 473,\ f_0^* = 1159\,\text{Hz}]$. In the second case, the matrix is a classic open cell foam of porosity with $\phi_m = 0.8$, $\mathcal{K}_m = 6.2 \times 10^{-8}\text{m}^2$, $\alpha_{m_\infty} \simeq 1$, thus $\omega_c = 25$ Hz, giving $\omega_0/\omega_c = 125 \times 10^5$ and a atypical band gap $[f_0 = 473,\ f_0^* = 603\,\text{Hz}]$. In both cases, the real part and absolute value of the velocity (divided by the sound velocity) and the attenuation factor, $At = \tan(\varphi)$, disclose the band gap effect ($A_t > 1$ means an attenuation higher than diffusion waves) and the possibility to reach supersonic velocity together with weak attenuation in a wide band of frequencies $f > f_0^*$.

V. CONCLUSION

Insert resonators in porous media leads to acoustic properties that depart from the classic poro-acoustic description. The study points out the key parameters of the system and explains the macroscopic behavior from the physics at the local scale, in the frequency range that respects the long wavelength condition. Despite similarities with meta-elastic materials or double porosity media, the particularity of the mechanisms driving the porous media with embedded resonators lead to a specific description.

In inner resonant porous media, two different pressure fields co-exist and interact dynamically at the scale of the period. This corresponds to a "co-dynamic" regime, in which macro wavelength and local resonance occur simultaneously. The key phenomenon relies on the fact that the elasto-inertial response of the resonator acts as a negative apparent stiffness that combines in series with the effective stiffness of the gas in the matrix. This results in an effective negative stiffness of the gas in the media, for frequencies belonging to a frequency band much wider than the close vicinity of the tuned frequency. The features of acoustic wave are drastically modified especially in this atypical band. According to the damping of the resonator, and to the nature of the flow regime in the matrix, one may obtain sharp broad band gap and band of low and high, up to supersonic, sound velocity: the lower is the matrix porosity, the wider is the band gap; the smaller is the resonator damping, the sharper is the band gap and the stronger is the dispersion.

The homogenized model is quasi-analytic, and its effective parameters are fully determined from the knowledge of the geometry and of the properties of the material constituting the period. Thus, the model can be used to project unconventional acoustic media. Inner resonant porous media could be of interest for practical applications, that may concern the design of new systems, either for damping or for fast/low velocity purpose, at different spatial and/or frequency scales. Finally, it would be of interest to realize such materials and to perform tests in order appreciate experimentally their actual properties.

[1]J.-L. Auriault and G. Bonnet, "Dynamique des composites élastiques périodiques" ("Dynamics of periodic elastic composites"), Arch. Mech. **37**(4–5), 269–284 (1985).
[2]J. O. Vasseur, P. A. Deymier, G. Prantziskonis, and G. Hong, "Experimental evidence for the existence of absolute acoustic band gaps in two-dimensional periodic composite media," J. Phys.: Condens. Mater **10**, 6051–6064 (1998).
[3]Z. Liu, X. Zhang, Y. Mao, Y. Y. Zhu, Z. Yang, C. T. Chan, and P. Sheng, "Locally resonant materials," Science **289**, 1734–1736 (2000).
[4]P. Sheng, X. X. Zhang, Z. Liu, and C. T. Chan, "Locally resonant sonic materials," Physica B **338**, 201–205 (2003).
[5]V. V. Zhikov, "On an extension of the method of two-scale convergence and its applications," Sbornick Mathematics **191**(7–8), 973–1014 (2000).
[6]A. Ávila, G. Griso, and B. Miara, "Bandes phoniques interdites en élasticité linéarisée" ("Phonic band gap in linear elasticity"), C. R. Acad. Sci. Paris, Ser. I **340**, 933–938 (2005).
[7]J.-L. Auriault, "Acoustics of heterogeneous media: Macroscopic behavior by homogenization," Curr. Topics Acoust. Res. **I**, 63–90 (1994).
[8]C. Boutin, P. Royer, and J. L. Auriault, "Acoustic absorption of porous surfacing with dual porosity," Int. J. Solids Struct. **35**(34–35), 4709–4737 (1998).
[9]X. Olny and C. Boutin, "Acoustic wave propagation in double porosity media," J. Acoust. Soc. Am. **113**(6), 73–89 (2003).
[10]E. Sanchez Palencia, *Nonhomogeneous Media and Vibration Theory, Lectures notes in Physics* (Springer-Verlag, Berlin, 1980), Vol. 127, 398 pp.
[11]J.-L. Auriault, C. Boutin, and C. Geindreau, *Homogenization of Coupled Phenomena in Heterogenous Media* (ISTE and Wiley, Hoboken, NJ, 2009), 476 pp.
[12]V. Tournat, V. Pagneux, D. Lafarge, and L. Jaouen, "Multiple scattering of acoustic waves and porous absorbing media," Phys. Rev. E **70**, 026609 (2004).
[13]C. Boutin, "Rayleigh scattering of acoustic wave in rigid porous media," J. Acoust. Soc. Am **12**(4), 1888–1905 (2007).
[14]L. Brillouin and M. Parodi, *Wave Propagation in Periodic Structures* (McGraw-Hill, New York, 1946), 272 pp.
[15]A. Krynkin, O. Umnova, Y. B. A. Chong, S. Taherzadeh, and K. Attenborough, "Scattering by coupled resonating elements in air," J. Phys. D **44**, 125101 (2011).
[16]H. Pichard, O. Richoux, and J.-P. Groby, "Experimental demonstrations in audible frequency range of band gap tunability and negative refraction in two-dimensional sonic crystal," J. Acoust. Soc. Am. **132**(4), 2816–2822 (2012).
[17]G. Allaire and C. Conca, "Bloch wave homogenization and spectral asymptotic analysis," J. Math. Pures Appli. **77**, 153–208 (1998).
[18]N. Turbe and C. Wilcox, "Application of Bloch expansion to periodic elastic and viscoelastic media," Math. Methods Appl. Sci. **4**(4–5), 433–449 (1982).
[19]M. Kafesaki and E. N. Economou, "Multiple-scattering theory for three-dimensional periodic acoustic composites," Phys. Rev. B **60**, 11993–12001 (1999).
[20]R. V. Craster, J. Klapunov, and A. V. Pichugin, "High-frequency homogenization for periodic media," Proc. R. Soc. A **466**, 2341 (2010).
[21]C. Boutin, A. Rallu, and S. Hans, "Large scale modulation of high frequency acoustics waves in periodic porous media," J. Acoust. Soc. Am. **132**(6), 3622–3636 (2012).
[22]J.-L. Auriault and C. Boutin, "Long wavelength inner-resonance cut-off frequencies in elastic composite materials," Int. J. Solid Struct. **49**, 3269–3281 (2012).

[23]R. Venegas and O. Umnova, "Acoustical properties of double porosity granular materials," J. Acoust. Soc. Am. **130**(5), 2765–2776 (2011).
[24]J. B. Pendry, A. J. Holden, D. J. Robbins, and W. J. Stewart, "Magnetism from conductors and enhanced nonlinear phenomena," IEEE Trans. Microwave Theory Tech. **47**, 2075–2084 (1999).
[25]J. F. Allard, *Propagation of Sound in Porous Media* (Elsevier Applied Science, New York, 1993), 284 pp.
[26]K. Attenborough, "Acoustical characteristics of rigid fibrous absorbents and granular media," J. Acoust. Soc. Am. **73**(3), 785–799 (1983).
[27]M. A. Biot, "Theory of propagation of elastic waves in a fluid-saturated porous solid. I. Low-frequency range," J. Acoust. Soc. Am. **28**, 168–178 (1956).
[28]M. A. Biot, "Theory of propagation of elastic waves in a fluid-saturated porous solid. II. Higher frequency," J. Acoust. Soc. Am. **28**, 179–191 (1956).
[29]Y. Champoux and J. F. Allard, "Dynamic tortuosity and bulk modulus in air saturated porous media," J. Appl. Phys. **70**, 1975–1979 (1991).
[30]C. Zwikker and W. Kosten, *Sound Absorbing Materials* (Elsevier, Amsterdam, 1949), Chap. 2, 300 pp.
[31]Z. Hashin, "Assessment of the self consistent scheme approximation: Conductivity of particulate composite," J. Comp. Mat. **2**, 284 (1968).
[32]J.-L. Auriault, "Dynamic behaviour of a porous medium saturated by a Newtonian fluid," Int. J. Eng. Sci. **18**, 775–785 (1980).
[33]J.-L. Auriault, L. Borne, and G. Chambon, "Dynamics of porous saturated media, checking of the generalized law of Darcy," J. Acoust. Soc. Am, **77**, 1641–1650 (1985).
[34]N. Fang, D. Xi, J. Xu, M. Ambati, W. Srituravanich, C. Sun, and X. Zang, "Ultrasonic meta-material with negative modulus," Nat. Mater. **5**, 452–456 (2006).
[35]C. Chesnais, C. Boutin, and S. Hans. "Effects of the local resonance on the wave propagation in periodic frame structures: Generalized Newtonian mechanics," J. Acoust. Soc. Am. **132**(4), 2873–2886 (2012).